5th International Conference on Experimental Fluid Mechanics ICEFM 2018 Munich
Munich, Germany, July 2-4, 2018

A calibration-free wall shear stress measurement technique using hot-film sensors

Xuanhe Liu, Zhuoyue Li, Nan Gao*

Dalian University of Technology, School of Aeronautics, Dalian, China

* gaonan@dlut.edu.cn

Abstract

Combined heat transfer and wall shear stress measurements on the inner wall of a fully developed turbulent air flow in a round pipe were presented in this note. The heat transfer was measured using a flush-mounted dual hot-film sensor composed of a non-electric conductive membrane sandwiched in between two thin Nickel films. Each of the two films was installed in a branch of a separate Kelvin bridge, and operated at a same temperature, the bottom film served as an active heat insulator so that the Joule heat from the upper film transferred only to the air. A calibration-free technique for wall shear stress measurement based only on the Joule heat flux was found to be feasible, providing the film temperature was sufficiently large.

1 Introduction

Heat transfer from a small isothermal hot-film strip mounted flush with an adiabatic wall to fluid was an age-old problem (Lévêque, 1928; Ludwieg, 1950; Liepmann and Skinner, 1954; Ling, 1963; Bellhouse and Schultz, 1966; Ackerberg et al., 1978). There was a renewed interest in this problem as the heat transfer rate Q was closely related to the wall shear stress τ_w, and can thus be utilized to quantify τ_w, as reviewed in Haritonidis (1989); Hanratty and Campbell (1996); Lofdahl and Gad-el-Hak (1999); Naughton and Sheplak (2002); Klewicki et al. (2007). The heat transfer process was complex as the temperature profiles were found to be different over the strip and an edge effect was large when the strip length was small (Ling, 1963). Based on the mass transfer measurement in liquids by Ackerberg et al. (1978) and the theory of Ling (1963), Haritonidis (1989) argued that the edge effects could be neglected when Péclet number ($Pe = l^{+2}Pr$) was larger than 100, Here, $l^+ = \rho u_\tau l/\mu$ was strip length l in terms of wall unit, and the friction velocity was $u_\tau = \sqrt{\tau_w/\rho}$. Analytical solutions of the energy equation were obtained under the assumptions of no edge effect ($Pe \geq 100$) and a linear velocity profile within the thermal boundary layer ($\delta_T^+ < 5$) (Liepmann and Skinner, 1954; Ludwieg, 1950) :

$$\overline{Nu}\, Pe^{-1/3} = 0.807. \tag{1}$$

or in a dimensional form (Bellhouse and Schultz, 1966; Liepmann and Skinner, 1954; Ludwieg, 1950)

$$Q = A\tau_w^{1/3}. \tag{2}$$

The sensitivity A was associated with the temperature difference between the film and and fluid, $\Delta T = T_u - T_o$, and properties of fluid. This was referred to as the classic $1/3$ power law (Hanratty and Campbell, 1996; Haritonidis, 1989; Lofdahl and Gad-el-Hak, 1999; Naughton and Sheplak, 2002), and was observed in many experimental investigations in both gas and liquid (Bellhouse and Schultz, 1966; Liepmann and Skinner, 1954; Ludwieg, 1950).

The $1/3$ power law represented by equations (1) and (2) can lead to a calibration-free wall stress measurement technique, in which τ_w can be estimated based only on the measurement of the heat transfer rate from the strip to fluid, Q, providing the two constraints discussed above were satisfied. However, Haritonidis Haritonidis (1989) argued $l^+ < 4.1Pr$ was needed for the second constraint ($\delta_T^+ < 5$) to be satisfied in the case of a turbulent boundary layer, which subsequently required $Pe < 5.8$ for the air flow ($Pr = 0.7$) that was in a contradiction of the first constraint of $Pe \geq 100$. The contradiction of the two constraints suggested the $1/3$ power law shall never be applied for air, that was obviously not true as its applicability was supported

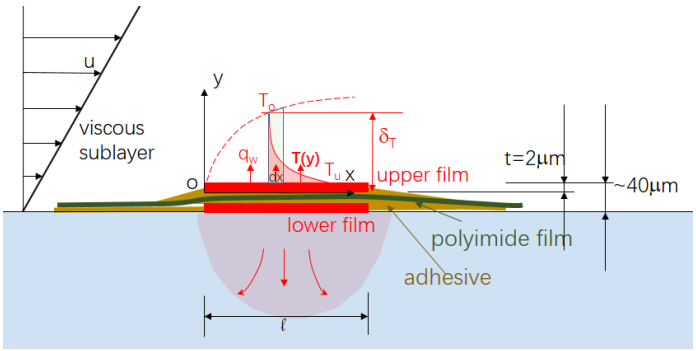

Figure 1: Schematic of the flush-mount dual hot-film sensor.

by many experiments, e.g. Bellhouse and Schultz (1966); Liepmann and Skinner (1954); Ludwieg (1950). Therefore, one or both of these two constraints should be loosened.

The calibration-free technique based on only the Joule heat Q is not practical due to a conduction heat loss to the wall, Q_s, as wall is not truly adiabatic in most applications and is hard to quantify and may change during experiment. Bellhouse and Schultz (1966) and other researchers, e.g. Hanratty and Campbell (1996); Haritonidis (1989); Lofdahl and Gad-el-Hak (1999); Naughton and Sheplak (2002), argued that the conduction heat loss was too complex to be modelled and thus a calibration was inevitable. Naughton and Sheplak (2002) pointed out that the impact of conduction heat loss was so large that it was hard to produce a unique calibration. The non-uniqueness of calibration prohibited the hot-film from being used as a reliable technique to quantify wall shear stress.

Inspired by the guard heater used in by Etrati et al. (2014); Osorio and Silin (2011), Liu et al. (2018) demonstrated the uniqueness of calibration could be achieved by using a dual hot-film sensor consisted of a non-electric conductive membrane sandwiched in between two metal films. The two films were operated at a same temperature with a difference within $\pm 0.2^oC$, and the conduction heat loss from the upper film to the wall was minimized to within 10% of the total Joule heat produced by that film. In their experiments, each film had four connection wires: the film temperature was set by supplying different current through the film using a pair of connection wires and its resistance was measured using another pair of wires. Furthermore, Liu et al. (2018) solved the energy equation applied to the thermal boundary layer and gave a relation between the Joule heat Q of the top film and the wall shear stress τ_w in an approach similar to Bellhouse and Schultz (1966). They gave an analytical model of the sensitivity A. Liu et al. (2018) tested the dual-film technique and their model in a long circular pipe for a constant film temperature and several Reynolds numbers and found the wall shear stresses measured using heat transfer without a calibration were within 15% of the true stresses, though maximum δ_T^+ in their experiment was as large as 16, much larger than the critical value of 5.

The calibration-free wall shear stress measurement technique proposed in Liu et al. (2018) appeared promising. Following their work, the effect of the film temperature was examined in this paper. The experimental methodology was given in the following section, followed by the results and discussions.

2 Experimental Methodology

The sensor used here was similar to that used by Liu et al. (2018). It was made of two $2\mu m$ thick $22.0mm$ wide (w) $1.75mm$ long (l) Nickel films (GOODFELLOW NI000120). The two thin films formed a sandwich structure separated by a $40mm$ long $40mm$ wide polyimide membrane (KAPTON 10) using adhesive, as shown in Fig. 1. The two edges of each film were connected to fine gauge copper wires by soldering, the effective length of the foil was approximately $20mm$. The length and width of both films were measured under a microscope at $40\times$ magnification with a uncertainty less than $\pm 0.01mm$. The polyimide membrane had a nominal thickness of $25\mu m$ but measurements with a micrometer suggested the average thickness was $d = 30\mu m$ with a uncertainty of $\xi_d = \pm 4.5\mu m$. The adhesive used here was Kafuter K704 silicone glue with a nominal thermal conductivity larger than $1.0W/mK$. The total thickness of adhesive (two layers) was less than $6\mu m$. The effect of adhesive on the conduction heat transfer was neglected as its thermal resistance was two orders of magnitude less than that of the polyimide membrane.

The film temperature can be adjusted by heating the film using different electric current. For example,

the upper film temperature T_u is related to its electric resistance R_u:

$$\Delta T = T_u - T_o = \frac{R_u - R_{uo}}{\alpha R_{uo}}. \tag{3}$$

Here, R_{uo} is the resistance of the upper film at the ambient temperature T_o, measured using a LCR gauge (KEYSIGHT E4980AL-032) with a uncertainty of $\xi_{R_{uo}}/R_{uo} \leq \pm 0.05\%$, and the temperature coefficient of resistance of Nickel is $\alpha = 0.0068^o C^{-1}$. The ambient temperature, T_o, was measured using a PT-100 temperature transducer with a uncertainty of $\xi_{T_o} = \pm 0.1^o C$. In practice, the upper and lower films were connected in a separate Kelvin bridge. The film temperatures were adjusted by manually modifying resistance of two potentiometers in each bridge, R_1 and R_2. The resistance of the other two potentiometers, R_3 and R_4, were set to equal to R_1 and R_2, respectively. The resultant R_u after the bridge reached a balance was

$$R_u = (R_2/R_1)R_n. \tag{4}$$

The uncertainties of the resistors, ξ_{R_1}/R_1, ξ_{R_2}/R_2 and ξ_{R_n}/R_n, were less than $\pm 0.01\%$. The uncertainty in R_u and R_l was evaluated using an approach outlined in Coleman and Steele Coleman and Steele (1998), e.g.

$$\xi_{R_u}^2 = \left(\frac{\partial R_u}{\partial R_1}\xi_{R_1}\right)^2 + \left(\frac{\partial R_u}{\partial R_2}\xi_{R_2}\right)^2 + \left(\frac{\partial R_u}{\partial R_n}\xi_{R_n}\right)^2. \tag{5}$$

Both ξ_{R_u}/R_u and ξ_{R_l}/R_l were less than $\pm 0.02\%$, and the uncertainties $\xi_{T_u-T_o}/(T_u - T_o)$ and xi_{T_u}/T_u were less than $\pm 0.05\%$ and $\pm 0.67\%$, respectively. These uncertainties were evaluated for a typical case with $T_u - T_o = 60^o C$ and $\tau_w = 0.5\,Pa$. It is noted that a filter was installed in the feedback loop to limit the response of the bridge as the thermal coupling between the two films made both bridges unstable. The bridges were stable after installing the filter and the typical response time of each bridge with the filter was $0.5\,s$.

The uncertainty of the conduction heat loss/gain through the polyimide substrate (ξ_{Q_s}) was determined by the uncertainty in temperature differences between the upper and lower films ($\xi_{T_u-T_l}$):

$$\xi_{Q_s} = k_p \frac{\xi_{T_u-T_l}}{d} lw, \tag{6}$$

where $k_p = 0.12 W/mK$ was the thermal conductivity of the polyimide membrane and d was its thickness, and

$$T_u - T_l = \frac{1}{\alpha}\left(\frac{R_u}{R_{uo}} - \frac{R_l}{R_{lo}}\right). \tag{7}$$

Combining the uncertainties in R_{uo}, R_u, R_{lo} and R_u, $\xi_{T_u-T_l}$ was found to be less than $\pm 0.15^o C$ for the typical case, thus ξ_{Q_s} was less than $\pm 0.025 W$.

The total Joule heat generated by the upper film was

$$Q_t = E^2/R_u = Q + Q_s + Q_r. \tag{8}$$

The voltage E was amplified by a factor of 10 and acquired directly using a 16-bit National Instruments PCI-6014 data acquisition card. The uncertainty in E was less than $\pm 0.1\%$ of the measured value, and thus the uncertainty ξ_{Q_t}/Q_t was less than $\pm 0.14\%$. Here, Q_s was taken as zero (the true conduction loss was not zero as $\xi_{Q_s} \neq 0$) and the radiation heat loss Q_r was evaluated using $Q_r = \varepsilon\sigma(T_u^4 - T_o^4)$. Here, emissivity $\varepsilon = 1$ and both T_u and T_o were in degree Kelvin. The radiation heat flux was less than 1% of Q in the typical case with. The uncertainty in Q was

$$\xi_Q^2 = \left(\frac{\partial Q}{\partial Q_t}\xi_{Q_t}\right)^2 + \left(\frac{\partial Q}{\partial Q_s}\xi_{Q_s}\right)^2 = \xi_{Q_t}^2 + \xi_{Q_s}^2, \tag{9}$$

thus ξ_Q/Q was less than $\pm 5.1\%$ in the case with $\Delta T \approx 60^o C$ and $\tau_w = 0.5\,Pa$, due primarily to the large ξ_{Q_s}. Properties of air, including k, c_p, μ, ν, ρ, were all evaluated using an averaged temperature of sensor film

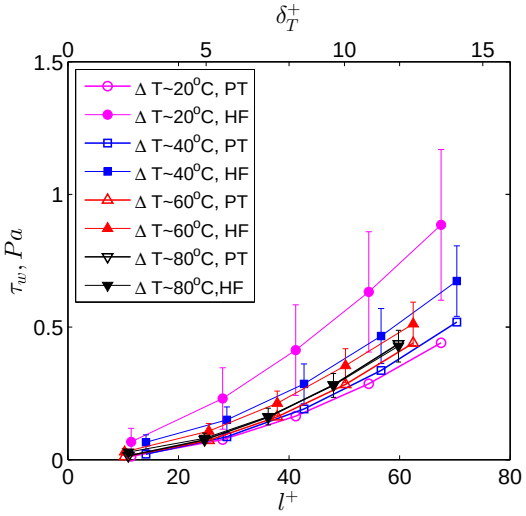

Figure 2: Distributions of the measured wall shear stress using the pressure transducer, $\tau_{w,PT}$, and those estimated using Joule heat of the upper film, $\tau_{w,HF}$, for different ΔT.

and air, $(T_u + T_o)/2$. Wall shear stress was also estimated using only the Joule heat from the upper hot-film, denoted by $\tau_{w,HF}$, using equations (3) and (4) in Liu et al. (2018):

$$\tau_{w,HF} = \left(1.33\frac{\mu}{k^2 \rho c_p w^3 l^2}\right)\left(\frac{Q}{\Delta T}\right)^3. \tag{10}$$

The uncertainty $\xi_{\tau_{w,HF}}/\tau_{w,HF}$ was more than 15.5% for the typical case, as it was over 3 times of the uncertainty of $Q/\Delta T$.

The dual hot-film sensor was attached to the inner wall near the exit of a long circular pipe, that was also used in Liu et al. (2018), where more details can be found. The difference was that the The mean static pressure at the tap (P) was measured using a pressure transducer (OMEGA ENGINEERING PX655) with a uncertainty of $\pm 0.31\,Pa$. The signal from the pressure transducer was acquired and averaged using a 16-bit National Instruments PCI-6014 data acquisition card with *LabView* routines. The sampling frequency was $1024\,Hz$ and the sampling time was 60 seconds. The time-averaged wall shear stress measured using the pressure transducer $\tau_{w,PT}$ (or τ_w for simplicity) was evaluated using

$$\tau_w = \frac{PD}{4L}. \tag{11}$$

Experiments were performed for Reynolds numbers ($Re_D = UD/\nu$) of 1.2×10^4 to 4.5×10^4. The averaged velocity in the pipe $U = 0.81U_{max}$, where U_{max} was measured using a pitot tube positioned at the center of the pipe exit and the same pressure transducer used in wall shear stress measurement. The constant 0.81 was determined by assuming the velocity profile could be described using a power-law equation with the exponent $n = 6.6$ (Hinze, 1975). The uncertainty in the measured τ_w was $\pm 1.1\%$ of measured value, for 95% confidence level. Following the measurements of wall shear stress, the film length in terms of wall unit was given by $l^+ = u_\tau l/\nu$, where the friction velocity was $u_\tau = \sqrt{\tau_w/\rho}$.

3 Results

The wall shear stress measured directly using pressure transducer and those computed using the heat transfer data $\tau_{w,HF}$ are shown in Fig. 2. When $\Delta T = 20^oC$, $\tau_{w,HF}$ was much larger than $\tau_{w,PT}$, and the differences were larger the uncertainty of $\tau_{w,HF}$ which were indicated using error bars. The error bars, as well as the differences between $\tau_{w,HF}$ and $\tau_{w,PT}$, became significantly smaller as ΔT increased. The differences between $\tau_{w,HF}$ and $\tau_{w,PT}$ were fairly small in the case of $\Delta T = 80^oC$ suggesting the wall shear stress obtained using the calibration-free method work fairly well here.

4 Conclusions

In this note we presented heat transfer measurements on the wall of a fully developed turbulent pipe flow using a newly developed dual hot-film sensor. Joule heat from the upper film can be used to predict τ_w using the equation 10. The uncertainties in the predicted $\tau_{w,HF}$ decreased as the film temperature $\Delta T = T_u - T_o$ increased to 80^oC, where the predicted and directly measured wall shear stress matched very well. This renders a promising direction for a calibration-free technique for wall shear stress measurement.

Acknowledgements

The research was funded by Natural Science Foundation of China (91752101,11572078) and 973 Plan (2014CB744100).

References

Ackerberg RC, Patel RD, and Gupta SK (1978) The heat/mass transfer to a finite strip at small Péclet numbers. *J Fluid Mech* 86:49–65

Bellhouse BJ and Schultz DL (1966) Determination of mean and dynamic skin friction, separation and transition in low-speed flow with a thin-film heated element. *J Fluid Mech* 24:379–400

Coleman H and Steele W (1998) *Experimentation and Uncertainty Analysis for Engineers, second ed.*. John Wiley & Sons, NY

Etrati A, Assadian E, and Bhiladvala R (2014) Analyzing guard-heating to enable accurate hot-film wall shear stress measurements for turbulent flows. *Int J Heat Mass Tran* 70:835 – 843

Hanratty T and Campbell J (1996) Measurement of wall shear stress. in R Goldstein, editor, *Fluid Mechanics Measurements*. chapter 11. CRC Press, Florida, US. 2 edition

Haritonidis J (1989) The measurement of wall shear-stress. in M Gad-el-Hak, editor, *Advances in fluid mechanics*. chapter 6, pages 229–261. Springer, Berlin

Hinze J (1975) *Turbulence, 2nd ed.*. McGraw-Hill, New York

Klewicki J, Saric W, Marusic I, and Eaton J (2007) Wall-bounded flows. in C Cameron, A Yarin, and J Foss, editors, *Handbook of Experimental Fluid Mechanics*. chapter 12, pages 871–902. Springer, Berlin

Lévêque A (1928) Les lois de la transmission de chaleur par convection. *Annales des Mines* 13:201–299, 305–362, 381–415

Liepmann H and Skinner G (1954) Shearing-stress measurements by use of a heated element. Technical Report TN-3268. NACA

Ling S (1963) Heat transfer from a small isothermal spanwise strip on an insulated boundary. *J Heat Transfer* 83:230–235

Liu X, Li Z, and Gao N (2018) An improved wall shear stress measurement technique using sandwiched hot-film sensors. *Theor Appl Mech Lett* 8:137 – 141

Lofdahl L and Gad-el-Hak M (1999) MEMS-based pressure and shear stress sensors for turbulent flows. *Meas Sci Technol* 10:665–686

Ludwieg H (1950) Instrument for measuring the wall shearing stress of turbulent boundary layers. Technical Report TM-1284. NACA

Naughton J and Sheplak M (2002) Modern developments in shear stress measurement. *Prog Aero Sci* 38:515–570

Osorio O and Silin N (2011) Wall shear stress hot film sensor for use in gases. in I Bove, C Cabeza, A Marti, and G Sarasua, editors, *Journal of Physics: Conference Series*. volume 296. page 012002. IOP Publishing